NASA TECHNICAL MEMORANDUM

NASA TM X-1558

NASA TM X-1558

CAPILLARY RISE IN THE ANNULAR REGION OF CONCENTRIC CYLINDERS DURING COAST PERIODS OF ATLAS-CENTAUR FLIGHTS

by Raymond F. Lacovic and James A. Berns

Lewis Research Center

Cleveland, Ohio

NATIONAL AERONAUTICS AND SPACE ADMINISTRATION • WASHINGTON, D. C. • MAY 1968

NASA TM X-1558

CAPILLARY RISE IN THE ANNULAR REGION OF CONCENTRIC CYLINDERS DURING COAST PERIODS OF ATLAS-CENTAUR FLIGHTS

By Raymond F. Lacovic and James A. Berns

Lewis Research Center
Cleveland, Ohio

NATIONAL AERONAUTICS AND SPACE ADMINISTRATION

For sale by the Clearinghouse for Federal Scientific and Technical Information
Springfield, Virginia 22151 – CFSTI price $3.00

CAPILLARY RISE IN THE ANNULAR REGION OF CONCENTRIC CYLINDERS DURING COAST PERIODS OF ATLAS-CENTAUR FLIGHTS

by Raymond F. Lacovic and James A. Berns

Lewis Research Center

SUMMARY

The Centaur space vehicle liquid oxygen and liquid hydrogen tanks each contain a mass sensing system which utilizes flow through a helical inlet tube into a probe consisting of two concentric cylinders. During the coast periods of the Atlas-Centaur flights, each mass sensing system acted as a capillary system under low gravity conditions. Data for the capillary rise height in the annular region of concentric cylinders as a function of time were obtained from the flights of three Atlas-Centaurs at acceleration levels of approximately 7.0×10^{-3} and 4.2×10^{-4} g with durations of up to 100 and 1341 seconds, respectively. The capillary rise data were correlated with an analytical expression which accurately described the fluid flow through the sensing system under low gravity conditions.

INTRODUCTION

In a satellite or space vehicle under a very low gravitational field, the capillary effect can be used to position liquids. Drop tower investigations by Petrash (ref. 1) and Siegel (ref. 2) have described the capillary effect and transient capillary rise for liquids into vertical tubes during a zero gravity period. These investigations, however, were necessarily limited to drop tower time durations (<3 sec) and to noncryogenic liquids.

During the low gravity coast periods of the Atlas-Centaur flights, the mass sensing probes for the liquid oxygen and liquid hydrogen tanks acted as capillary systems and provided an opportunity to extend the data of references 1 and 2 to considerably longer periods of time and to the use of cryogenic fluids. The geometry of the Centaur mass sensing probes, the acceleration levels of the Centaur vehicle, and the duration of the coast period were such that a complete transient capillary rise rate profile from start to

steady-state conditions was nearly provided. An analytical investigation was conducted at the Lewis Research Center in order to correlate the capillary rise data of the concentric tube configuration and the environment of the mass sensing probes with known fluid flow principles. The results of the analysis, which accounts for the pressure losses that occur throughout the fluid, are presented herein.

SYMBOLS

A	area, m^2
F_s	surface tension force
F_T	total force
g	acceleration, m/sec^2
K_1	inlet tube entrance loss coefficient
K_2	inlet tube helical shape correction term coefficient
K_3	inlet tube exit loss coefficient
L	annulus liquid level, m
l	tube length, m
ΔP_a	acceleration pressure loss, N/m^2
ΔP_{EA}	inlet tube exit pressure loss, N/m^2
ΔP_{EI}	inlet tube entrance pressure loss, N/m^2
ΔP_{FA}	frictional pressure loss in annulus, N/m^2
ΔP_{FI}	frictional pressure loss in inlet tube, N/m^2
P_s	surface tension pressure, N/m^2
P_u	ullage pressure, N/m^2
r	radius, m
Z	capillary rise height, m
$\dot{Z}$	capillary rise liquid velocity, m/sec
$\ddot{Z}$	capillary rise liquid acceleration, m/sec^2
β	r_{ic}/r_{oc}
θ	contact angle between liquid and solid, rad
μ	viscosity, $(N)(sec)/m^2$

ρ liquid density, kg/m^2

σ surface tension, N/m

Subscripts:

A annulus

C Centaur tank

I inlet tube

ic inner cylinder

oc outer cylinder

EXPERIMENTAL DESCRIPTION

The Centaur space vehicle utilized two acceleration levels during the coast period of the Atlas-Centaur 8, 9, and 12 flights (designated AC-8, AC-9, and AC-12, respectively). The acceleration levels and their durations are given in table I.

TABLE I. - CENTAUR COAST PERIOD

ACCELERATION LEVELS

Flight	Acceleration level 1, g	Duration of acceleration level 1, sec	Acceleration level 2, g	Duration of acceleration level 2, sec
AC-8	7.15×10^{-3}	100	4.28×10^{-4}	820
AC-9	7.15	76	4.28	1341
AC-12	6.90	76	4.15	1214

The first acceleration level is applied after Centaur first main engine cutoff in order to reduce the propellant disturbances associated with main engine thrust termination. The second, lower, acceleration level is employed to maintain the propellants at the rear of the tank (for engine restart) throughout the coast period. A complete description and analysis of the use of these acceleration levels for the coast period of AC-8 is given in reference 3.

The Centaur space vehicle utilizes a mass sensing probe in the liquid hydrogen and liquid oxygen tanks to regulate the mixture ratio of the propellants during main engine

firing. Each mass sensing probe consists, in part, of concentric cylinders with a helical inlet tube.

A schematic of the mass sensing probes, together with a listing of the probe dimensions, is shown in figure 1. As shown in the figure, saturated liquid enters the helical inlet tube and passes into the annular region. As the liquid rises in the annular region, the capacitance changes between the two plates. The change in capacitance is telemetered to a ground station providing a continuous reading of the varying mass in the probe. Since the probe calibration in terms of mass and capacitance and the annular cross-sectional area of the probe are known, the liquid level in the annular region is easily determined. Hence, the transient liquid level rise in the annular region of concen-

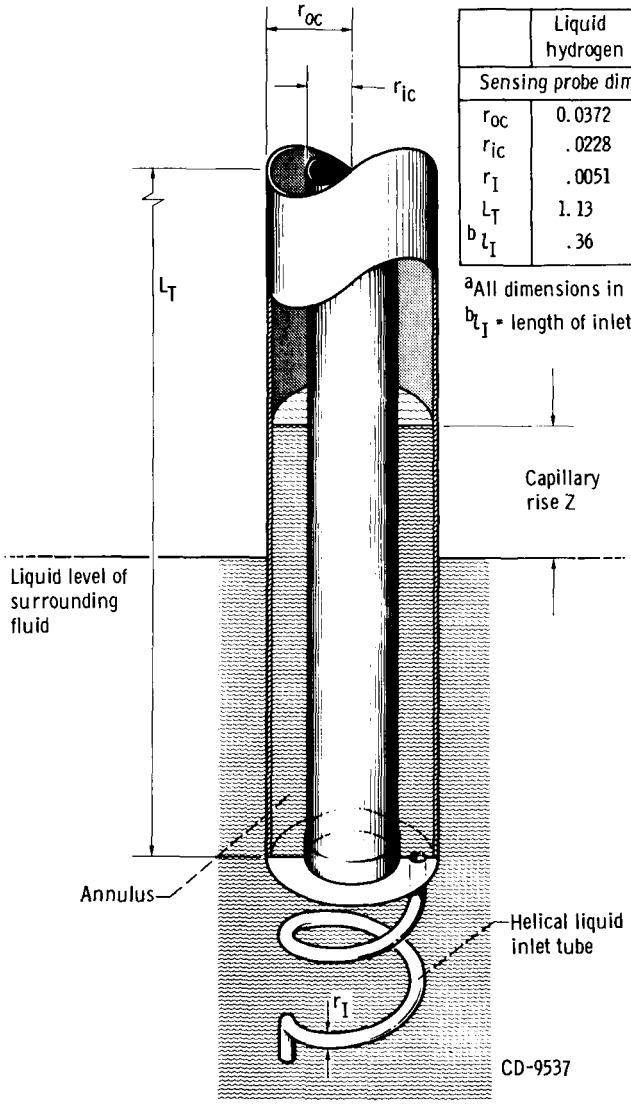

	Liquid hydrogen	Liquid oxygen
Sensing probe dimensions[a]		
r_{oc}	0.0372	0.0595
r_{ic}	.0228	.0473
r_I	.0051	.0046
L_T	1.13	.49
[b] L_I	.36	.51

[a] All dimensions in meters.

[b] L_I = length of inlet tube.

Figure 1. - Schematic of Centaur liquid hydrogen and liquid oxygen mass sensing probes.

tric cylinders was obtained for the two Centaur coast period acceleration levels.

ANALYSIS

It is suggested in references 1 and 2 that in order to predict analytically the transient movement of liquids into vertical capillaries the pressure losses that occur anywhere in the fluid must be taken into account. For the particular geometry of the Centaur liquid oxygen and liquid hydrogen mass sensing probes, the various pressure losses are indicated in figure 2. The summation of these pressure losses for the capillary rise in the annular region can be expressed as follows:

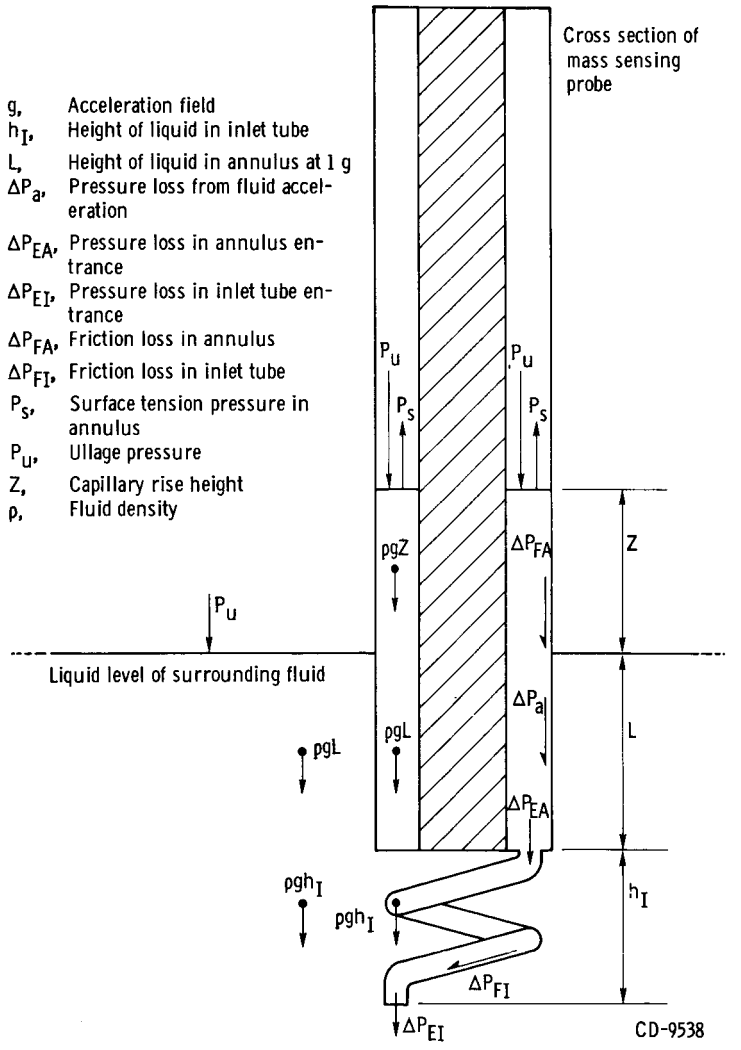

Figure 2. - Summation of pressures for capillary rise in annular region of concentric cylinder mass sensing probe.

$$P_u + \rho g h_I + \rho g L = P_u + \rho g Z + \rho g L + \rho g h_I + \Delta P_{FA} + \Delta P_{EA} + \Delta P_{FI} + \Delta P_{EI} + \Delta P_a - P_s$$

Then,

$$P_s - \Delta P_{EI} - \Delta P_{FI} - \Delta P_{EA} - \Delta P_{FA} - \Delta P_a - \rho g Z = 0 \tag{1}$$

Each pressure term will now be defined.

Surface Tension Pressure P_s

The effects of surface tension on liquid rising in an annulus has been investigated by Seebold (ref. 4). He has shown that, in a low gravity environment, the interface advances faster on one wall than the other and that the distortion of the interface is a function of Bond number and annular radii ratio r_{ic}/r_{oc}. For the case at hand, both the experimental data and that of reference 4 indicate this distortion was negligible so that a radially symmetric curved interface may be assumed with little error.

The summation of the surface tension forces around the annulus perimeter is

$$F_s = 2\pi(r_{ic} + r_{oc})\sigma \cos\theta$$

Dividing each side by the annulus area A_A results in the pressure due to surface tension

$$\frac{F_s}{A_A} = P_s = \frac{2\pi(r_{ic} + r_{oc})\sigma \cos\theta}{\pi\left(r_{oc}^2 - r_{ic}^2\right)} = \frac{2\sigma \cos\theta}{r_{oc} - r_{ic}} \tag{2}$$

Inlet Tube Entrance Loss ΔP_{EI}

At the entrance to the inlet tube a pressure loss results from the momentum changes necessary to form the velocity profile. The entrance loss is expressed as (ref. 5)

$$\Delta P_{EI} = \frac{K_1}{2}\rho(\dot{Z}_I)^2 = \frac{K_1}{2}\rho(\dot{Z}_A)^2\left(\frac{A_A}{A_I}\right)^2 \tag{3a}$$

where (ref. 5)

$$K_1 = 0.4\left(1.25 - \frac{A_I}{A_C}\right) \tag{3b}$$

When the entrance loss is expressed in terms of the annulus fluid velocity, equation (3a) can be expressed as

$$\Delta P_{EI} = \frac{K_1}{2} \rho \dot{Z}_A^2 \left(\frac{r_{oc}^2 - r_{ic}^2}{r_I^2}\right)^2 \tag{4}$$

For the Centaur vehicle, $A_I/A_C \approx 0$. Then, from equation (3b), $K_1 = 0.5$.

Inlet Tube Drag Loss ΔP_{FI}

As the fluid passes through the inlet tube frictional losses will occur. These losses can be expressed from the Hagan-Poiseville relation as (ref. 6)

$$\Delta P_{FI} = \frac{8 \mu l_I \dot{Z}_I}{r_I^2} K_2 \tag{5}$$

where K_2 is a correction term for the helical inlet tube shape. When the inlet tube drag loss is expressed in terms of the annular fluid velocity, equation (5) can be expressed as

$$\Delta P_{FI} = 8 \frac{\mu l_I}{r_I^2} \dot{Z}_A K_2 \left(\frac{r_{oc}^2 - r_{ic}^2}{r_I^2}\right) \tag{6}$$

where K_2 for the helical inlet tubes using cryogenic fluids is approximately 1 (ref. 5).

Inlet Tube Exit Loss ΔP_{EA}

As the fluid enters the annular region from the inlet tube, a pressure loss due to expansion will occur. This pressure loss can be expressed as (ref. 5)

$$\Delta P_{EA} = \frac{1}{2} \dot{Z}_I^2 \left(1 - \frac{A_I}{A_A}\right)^2 \rho \tag{7}$$

or in terms of the annular fluid velocity

$$\Delta P_{EA} = \frac{1}{2} \dot{Z}_A^2 K_3 \left(\frac{r_{oc}^2 - r_{ic}^2}{r_I^2}\right)^2 \rho \tag{8}$$

where

$$K_3 = \left(1 - \frac{A_I}{A_A}\right)^2$$

Annulus Drag Loss ΔP_{FA}

As the fluid passes through the annulus, a frictional loss with the cylinder walls will occur. The frictional loss in the annulus can be expressed as a modified form of the Hagan-Poiseville equation (ref. 6)

$$P_{FA} = 8 \frac{\mu(L + Z)}{r_{oc}^2} \dot{Z}_A \left(\frac{1 - \beta^4}{1 - \beta^2} - \frac{1 - \beta^2}{\ell n \frac{1}{\beta}}\right) \tag{9}$$

where $\beta = r_{ic}/r_{oc}$.

Acceleration Losses ΔP_a

As the fluid is accelerated through the inlet tube and the annular region, a pressure loss due to fluid acceleration occurs. This pressure loss can be derived from Newton's force-mass relation as follows:

$$F_T = m_I \ddot{Z}_I + m_A \ddot{Z}_A$$

$$F_T = l_I \rho A_I \ddot{Z}_I + (L + Z)\rho A_A \ddot{Z}_A$$

$$\Delta P_a = \frac{l_I \rho A_I}{A_I} \ddot{Z}_I + (L + Z)\rho \frac{A_A}{A_A} \ddot{Z}_A$$

or, in terms of the annular fluid acceleration,

$$\Delta P_a = l_I \rho \ddot{Z}_A \left(\frac{A_A}{A_I}\right) + (L + Z)\rho \ddot{Z}_A$$

$$\Delta P_a = \rho \ddot{Z}_A \left(L + Z + l_I \frac{A_A}{A_I}\right)$$

$$\Delta P_a = \rho \ddot{Z}_A \left[L + Z + l_I \left(\frac{r_{oc}^2 - r_{ic}^2}{r_I^2}\right)\right] \tag{10}$$

The substitution of the expressions obtained for the various pressure losses into equation (1) yields the following equation:

$$\frac{2\sigma \cos\theta}{r_{oc} - r_{ic}} - \frac{K_1}{2} \rho \dot{Z}_A^2 \left(\frac{r_{oc}^2 - r_{ic}^2}{r_I^2}\right)^2 - 8 \frac{\mu l_I \dot{Z}_A}{r_I^2} K_2 \left(\frac{r_{oc}^2 - r_{ic}^2}{r_I^2}\right) - \frac{\rho}{2} \dot{Z}_A^2 K_3 \left(\frac{r_{oc}^2 - r_{ic}^2}{r_I^2}\right)^2$$

$$- 8 \frac{\mu(L + Z)}{r_{oc}^2} \dot{Z}_A \left(\frac{1 - \beta^4}{1 - \beta^2} - \frac{1 - \beta^2}{\ln \frac{1}{\beta}}\right)^{-1} - \rho \ddot{Z}_A \left[L + Z + l_I \left(\frac{r_{oc}^2 - r_{ic}^2}{r_I^2}\right)\right] - \rho g Z = 0 \tag{11}$$

At steady-state conditions, equation (11) reduces to

$$\frac{2\sigma \cos\theta}{r_{oc} - r_{ic}} - \rho g Z = 0 \tag{12}$$

Equation (11) was solved for the acceleration $\ddot{Z}_A$, the velocity $\dot{Z}_A$, and the displacement Z in the annular region as a function of time by successive integrations on a high speed IBM 7094 computer. The Runge-Kutta method of forward integration was used.

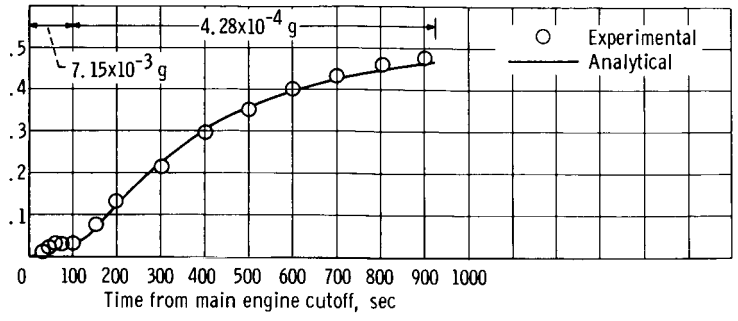

(a) AC-8.

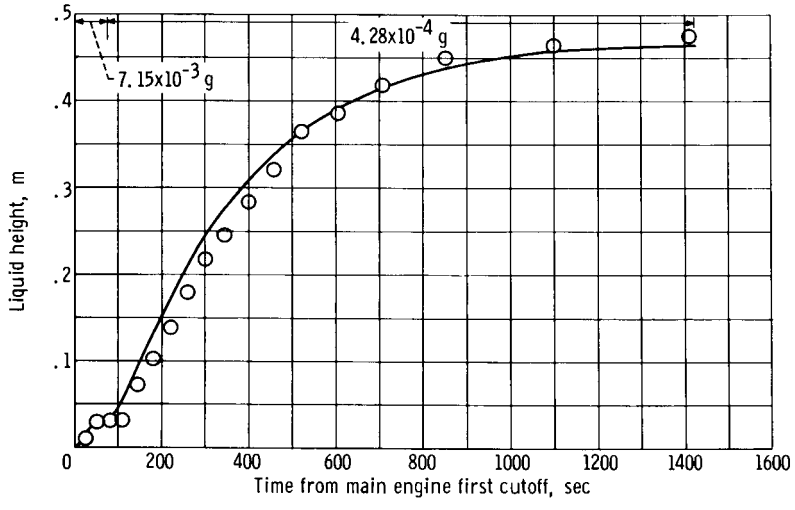

(b) AC-9.

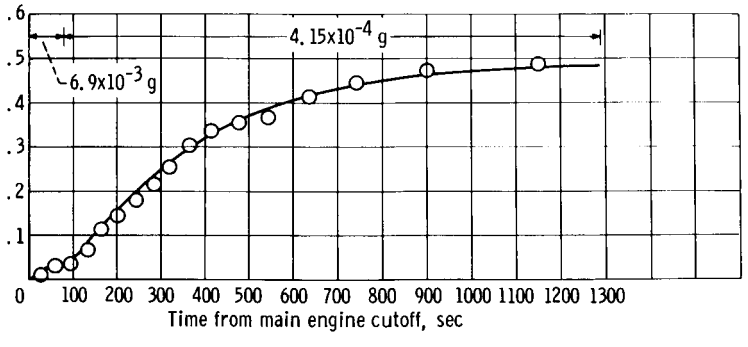

(c) AC-12.

Figure 3. - Liquid oxygen capillary rise.

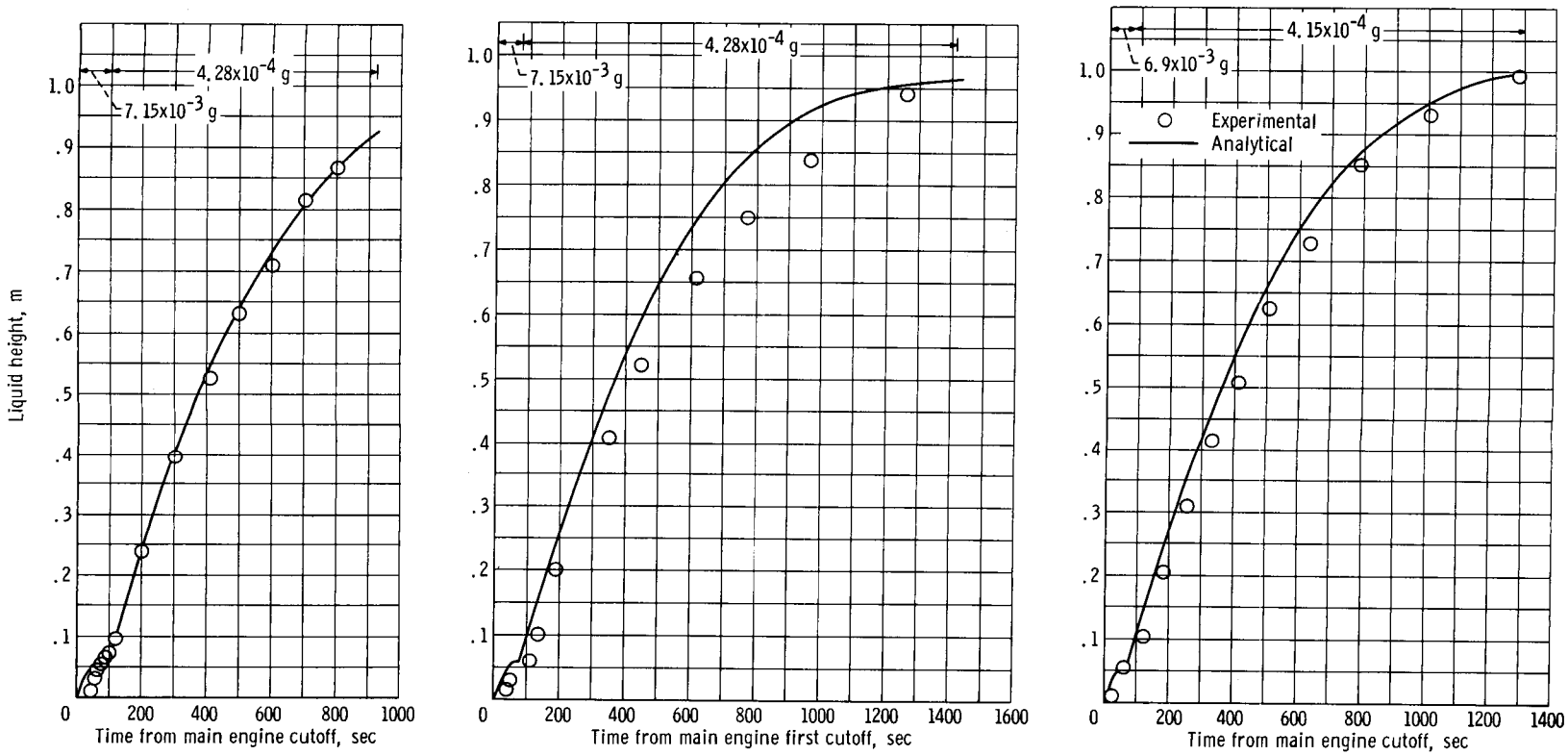

(a) AC-8.

(b) AC-9.

(c) AC-12.

Figure 4. - Liquid hydrogen capillary rise.

RESULTS AND DISCUSSION

The capillary liquid level rise in the annular region of the concentric cylinder liquid oxygen and liquid hydrogen mass sensing probes obtained from the coast phase data of AC-8, AC-9, and AC-12 flights is presented in figures 3 and 4. The data are estimated to be accurate to within ±15 percent for the high acceleration level.

The transition in acceleration level that occurred at 100 seconds for AC-8 and at 76 seconds for AC-9 and AC-12 after main engine cutoff is indicated in each figure by the break in slope of the capillary liquid level rise. The effect of the acceleration level on the steady-state liquid levels is clearly shown in each figure. The greater acceleration level results in a lower steady-state liquid level. A comparison of figures 3 and 4 also indicates the effect of fluid properties on the capillary rise and steady-state liquid levels. The lower density liquid hydrogen (fig. 4) rises at a greater rate to a steady-state liquid level; the rate is nearly twice that observed with those obtained from the derived analytical expression (eq. (11)). Generally, the theoretical curve agrees very favorably with the experimental liquid oxygen liquid levels. The liquid hydrogen liquid level rise appears to be slightly delayed in initial response to the acceleration change, compared to the theoretical curve. The steady-state liquid levels predicted from equation (12) at the two acceleration levels are compared to the actual steady-state values in table II. Examination of table II reveals that the predicted steady-state liquid levels agree favorably with the actual steady-state liquid levels.

TABLE II. - STEADY-STATE LIQUID LEVELS

Flight	Acceleration level, g	Actual steady-state liquid level, m		Predicted steady-state liquid level, m	
		LOX tank	LH_2 tank (a)	LOX tank	LH_2 tank
AC-8	7.15×10^{-3}	0.03	0.07	0.03	0.06
AC-9	7.15	.03	.06	.03	.06
AC-12	6.90	.03	.06	.04	.07
AC-8	4.28	[a].48	.97	.47	.97
AC-9	4.28	.48	.98	.47	.97
AC-12	4.15	.50	1.00	.49	1.00

[a]Based on extrapolated data.

SUMMARY OF RESULTS

During the coast period of the Atlas-Centaur flights, the liquid hydrogen and liquid oxygen concentric cylinder mass sensing systems acted as capillary systems under low gravity conditions. Data for the capillary rise height in the annular region of a concentric cylinder as a function of time was obtained from the flights for acceleration levels of approximately 7.0×10^{-3} and 4.2×10^{-4} g. The duration of these acceleration periods were up to 100 and 1341 seconds, respectively, and were of sufficient duration to nearly provide a transient capillary rise profile from start to steady-state conditions.

The capillary liquid level rise data were correlated with an analytical expression derived from a balance of fluid pressure losses. The analytical expression correlated well with the actual flight data and accurately described the fluid flow through the sensing system under low gravity conditions.

Lewis Research Center,
National Aeronautics and Space Administration,
Cleveland, Ohio, January 10, 1968,
891-01-00-06-22.

REFERENCES

1. Petrash, Donald A.; Nelson, Thomas M.; and Otto, Edward W.: Effect of Surface Energy on the Liquid-Vapor Interface Configuration During Weightlessness. NASA TN D-1582, 1963.

2. Siegel, Robert: Transient Capillary Rise in Reduced and Zero-Gravity Fields. J. Appl. Mech., vol. 83, no. 2, June 1961, pp. 165-170.

3. Lacovic, Raymond F.; Yeh, Frederick C.; Szabo, Steven V., Jr.; Brun, R. J.; Stofan, Andrew J.; and Berns, James A.: Management of Cryogenic Propellants in a Full-Scale Orbiting Space Vehicle. NASA TN D-4571, 1968.

4. Seebold, J. G.; Hollister, M. P.; Satterlee, H. M.: Capillary Hydrostatics in Annular Tanks. Paper No. 66-425, AIAA, June 1966.

5. Perry, John H., ed.: Chemical Engineers' Handbook. Third ed., McGraw-Hill Book Co., Inc., 1950.

6. Bird, R. Byron; Stewart, Warren E.; and Lightfoot, Edwin N.: Transport Phenomena. John Wiley & Sons, Inc., 1960.